

CER 72-73 PJW20

PLASMA PROPERTY CONTOURS IN  
A 15 CM HOLLOW CATHODE KAUFMAN THRUSTER

Work performed under  
GRANT NGR-06-002-112  
LEWIS RESEARCH CENTER  
NATIONAL AERONAUTICS AND SPACE ADMINISTRATION

Paul J. Wilbur  
Jerry Isaacson

February 1973  
Department of Mechanical Engineering  
Colorado State University  
Fort Collins, Colo.



U18401 0073550

## TABLE OF CONTENTS

Introduction	1
Apparatus and Procedure	1
Langmuir Probe System Circuitry	2
Langmuir Probes	3
Results	4
Thruster Operating Conditions	5
Plasma Property Contours	8 through 19
References	20

## INTRODUCTION

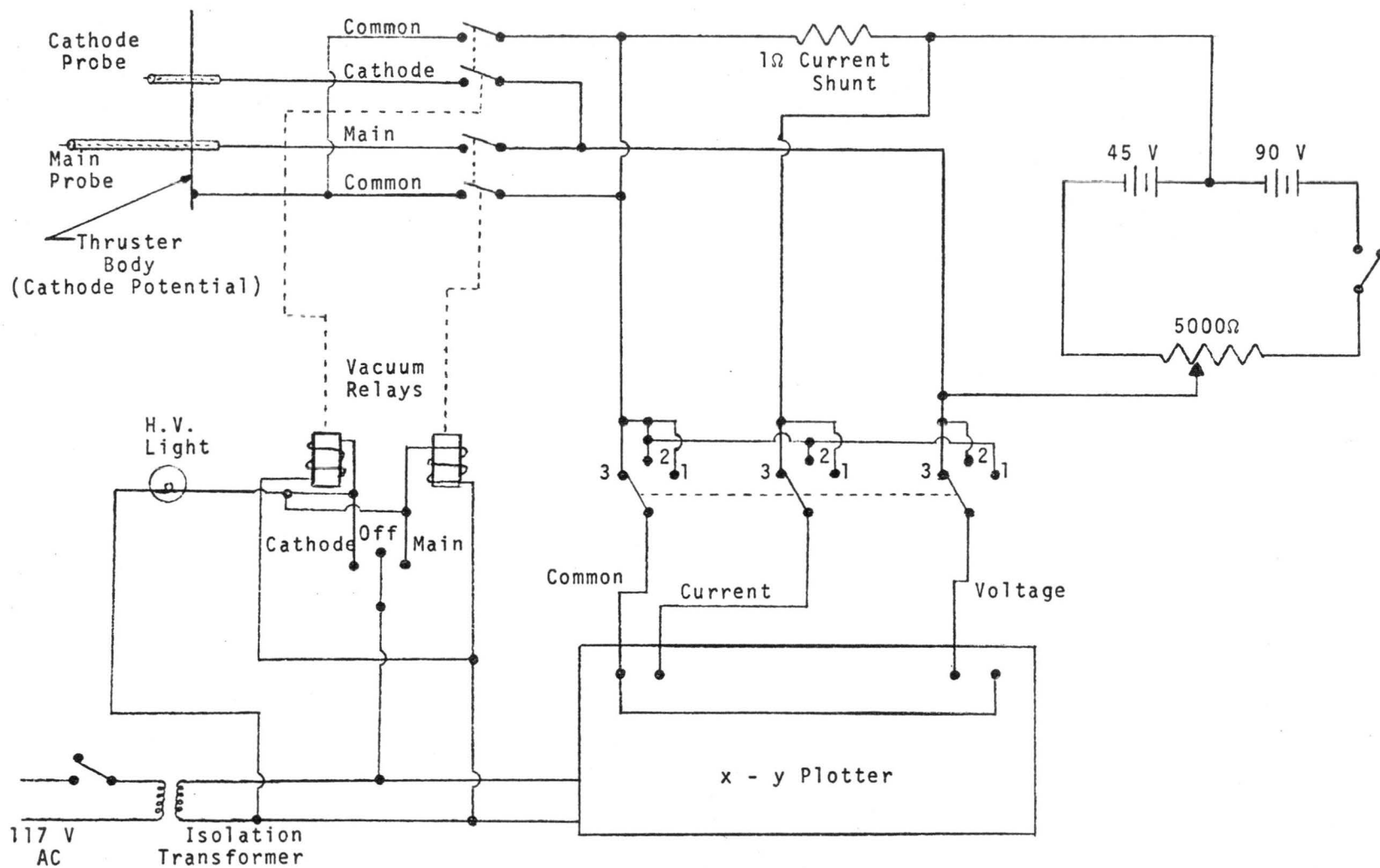
As part of an effort to understand plasma phenomena inherent to electron bombardment ion thruster operation, extensive Langmuir probing of the main and cathode discharge regions of a 15 cm dia thruster has been conducted. The effects of adjustment in cathode pole piece dimensions, flow rates and grid system perveance on plasma properties have been investigated.

## APPARATUS AND PROCEDURE

The thruster on which the work described herein was performed is a 15 cm dia SERT II unit which had been modified to permit: 1) independent control and measurement of mercury flow rates to the neutralizer, hollow cathode, and main propellant distributor and 2) variation of magnetic field intensity. The details of the thruster modification as well as power and measurement systems descriptions are given in reference 1.

Two Langmuir probes installed in the thruster were used to record traces from which plasma properties could be determined. These data were recorded through the circuitry shown in Figure 1 on the 11 in. x 14 in. recording surface of an x-y plotter. Traces were evaluated in the manner suggested by Strickfaden and Geiler<sup>2</sup>. The Langmuir probes were designed so they could be swept through a semicircular arc and moved axially to survey either the entire main or cathode discharge region during thruster operation as suggested by the sketches of Figure 2.

FIGURE 1.



LANGMUIR PROBE SYSTEM CIRCUITRY

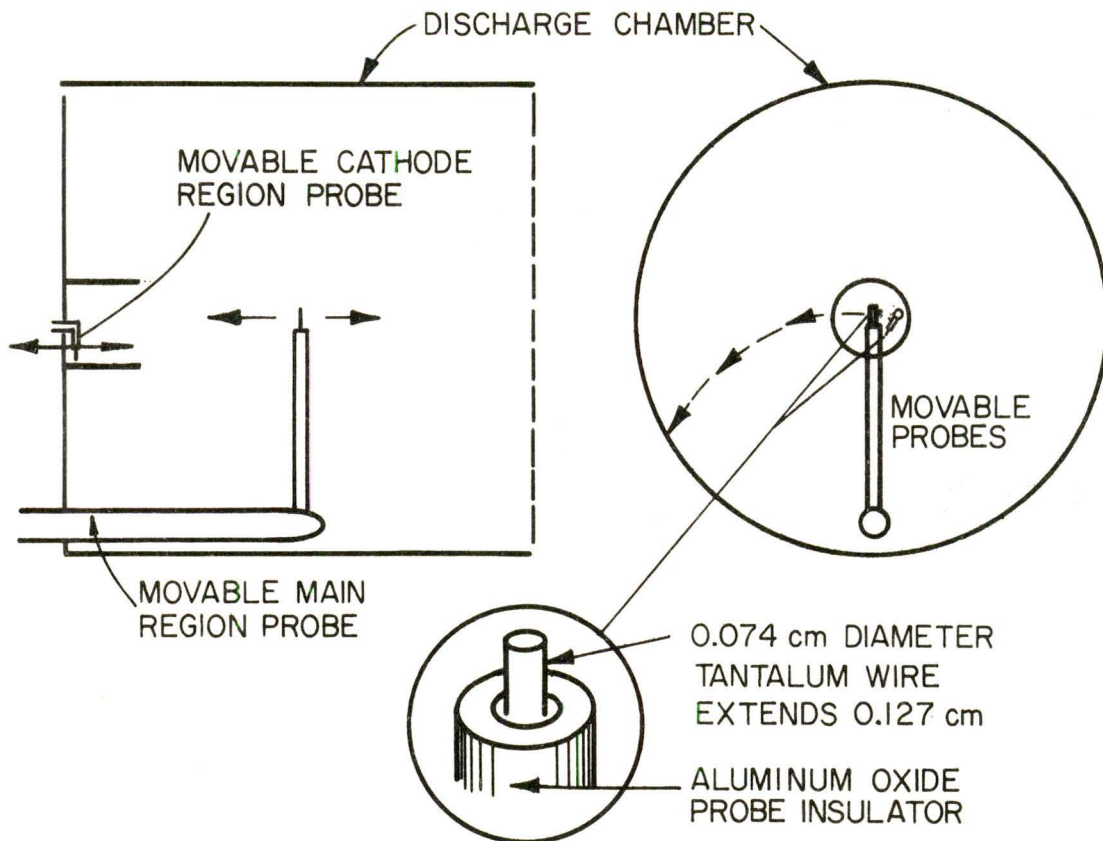


FIGURE 2. LANGMUIR PROBES

On each of these plots, the location of the forward edge of the cathode pole piece is identified. Figures 8 through 14 are all main discharge region contours.

The following conclusions are suggested by a review of these data:

A. Cathode Region

1. The plasma potential rises to a substantial fraction of anode potential in the vicinity of the baffle aperture.
2. Electron temperature tends to arise rather abruptly near the baffle aperture. Investigation of Langmuir probe data near the aperture suggests however that the electrons are becoming non-maxwellian due to acceleration in this region and the apparent increase in electron temperature is a manifestation of the associated increase in energy.
3. Cathode region conditions are not affected markedly by changes in cathode flow rate, but are affected by variations in arc current.

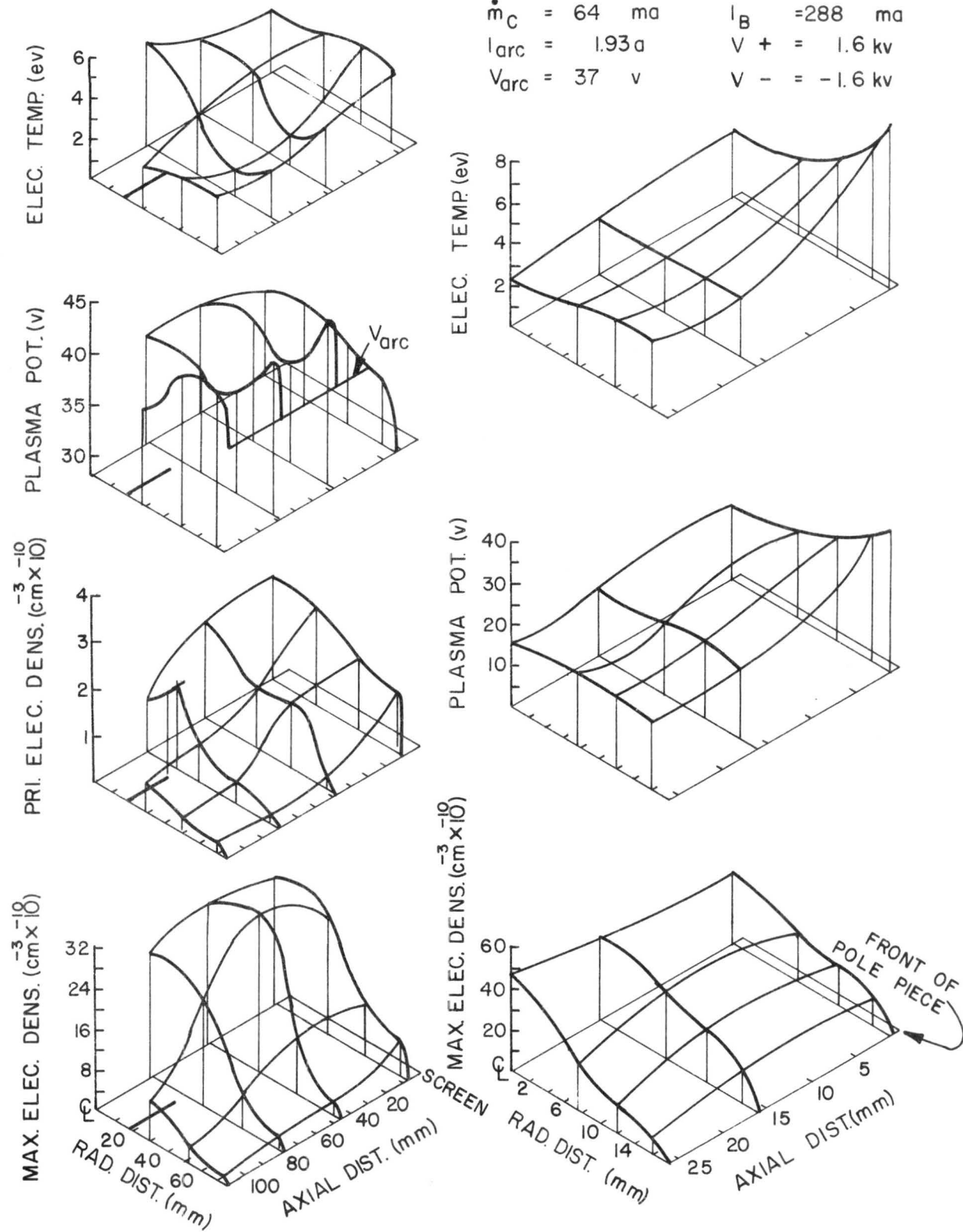
B. Main Discharge Region

1. Plasma Potential in the main discharge region tends to be above the anode potential, and there is a plasma potential ridge adjacent to the anode in general. These conditions are presumed to exist because of the magnetic field which suppresses electron migration to the anode and results therefore in a slightly elevated ion density near the anode which causes the observed plasma potential ridge.
2. The primary electron radial density profile near the

screen grid tends to be much flatter than the maxwellian electron density profile at the same location for a thruster with a properly designed magnetic field. When the cathode pole piece is extended or reduced in diameter and the magnetic field is altered the primary electron density profile at the grids tends to become more peaked.

3. Primary electron densities tend to be higher when dished high perveance grid systems are employed.
4. As the thruster is throttled, the maxwellian electron density drops markedly and the primary electron density remains essentially constant.

$\dot{m}_T = 440 \text{ ma}$   
 $\dot{m}_C = 64 \text{ ma}$   
 $I_{arc} = 1.93 \text{ a}$   
 $V_{arc} = 37 \text{ v}$   
 $I_B = 288 \text{ ma}$   
 $V_+ = 1.6 \text{ kv}$   
 $V_- = -1.6 \text{ kv}$



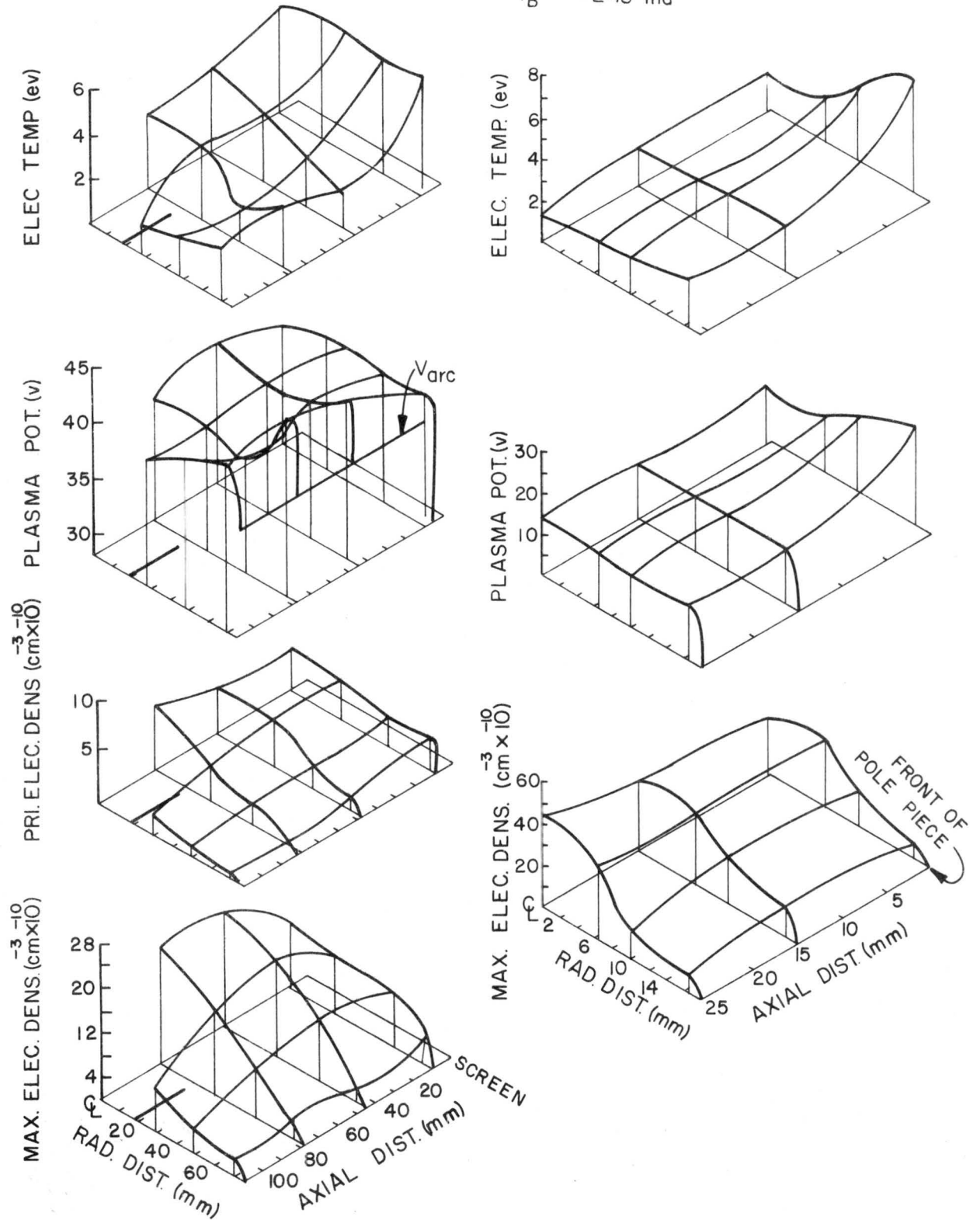
a. Main Region

b. Cathode Region

FIGURE 3.



$\dot{m} = 440 \text{ ma}$      $V_{\text{arc}} = 37 \text{ v}$   
 $\dot{m} = 57 \text{ ma}$      $V_+ = 1.6 \text{ kv}$   
 $I_{\text{arc}} = 1.6 \text{ a}$      $V_- = -1.6 \text{ kv}$   
 $I_B = 245 \text{ ma}$



a. Main Region

b. Cathode Region

FIGURE 4.

$$\dot{m}_T = 440 \text{ ma}$$

$$\dot{m}_C = 91 \text{ ma}$$

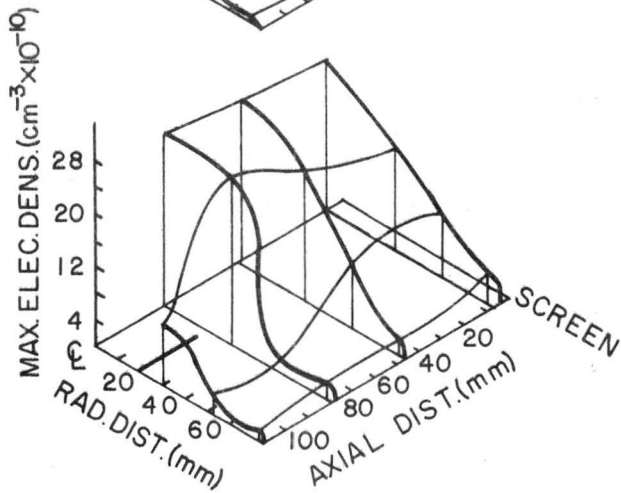
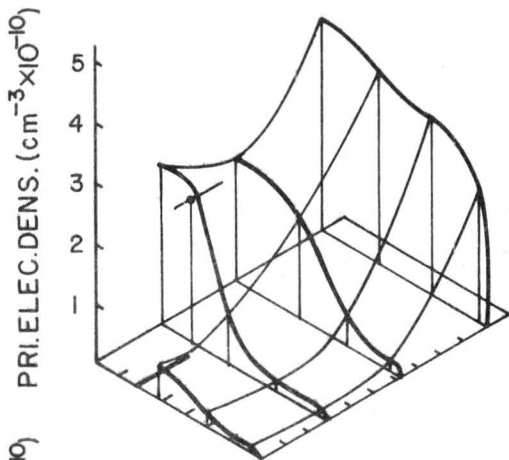
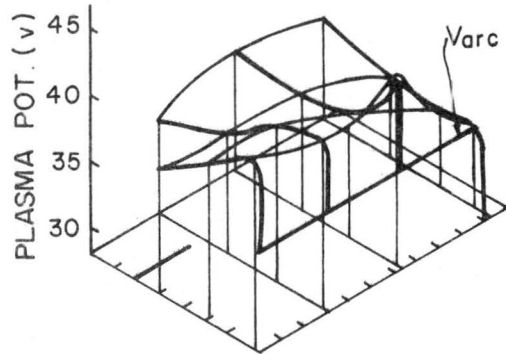
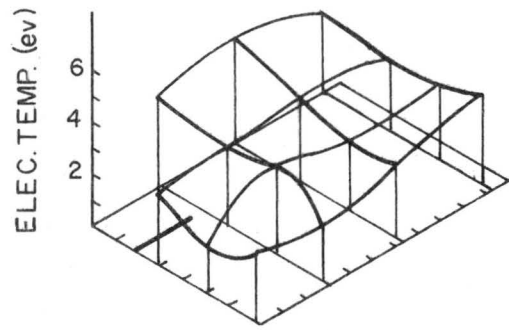
$$I_{arc} = 1.92 \text{ a}$$

$$V_{arc} = 37 \text{ v}$$

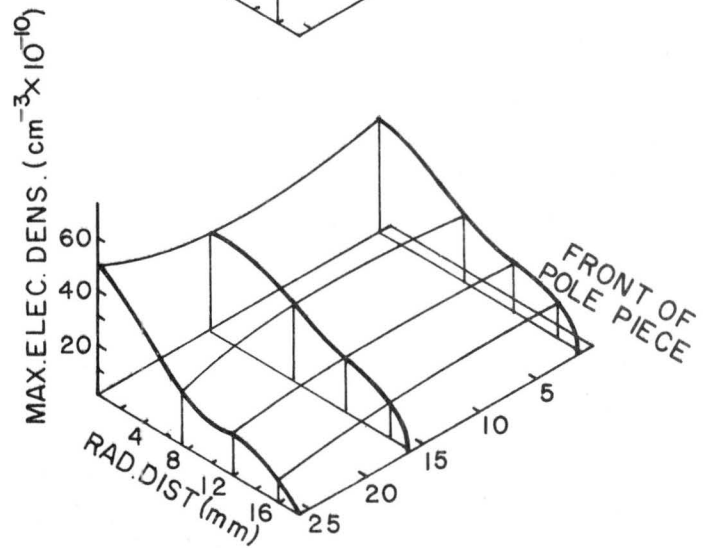
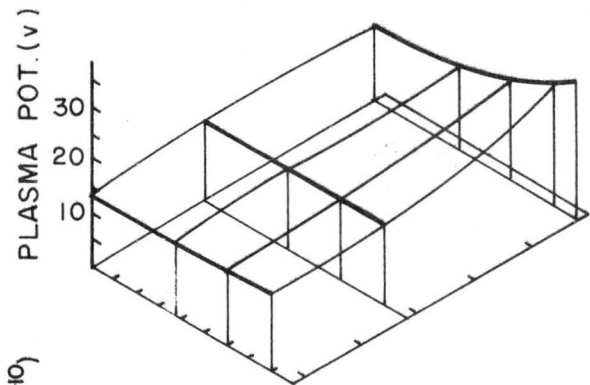
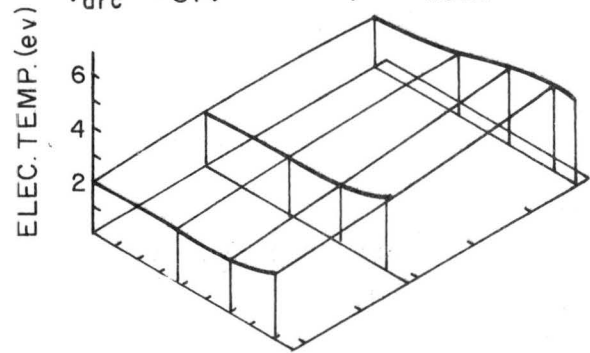
$$I_B = 284 \text{ ma}$$

$$V_+ = 1.6 \text{ kv}$$

$$V_- = -1.6 \text{ kv}$$



a. Main Region



b. Cathode Region

FIGURE 5.

$\dot{m}_T = 220 \text{ ma}$   
 $\dot{m}_C = 71 \text{ ma}$        $I_B = 176 \text{ ma}$   
 $I_{arc} = 1.09 \text{ a}$        $V_+ = 1.6 \text{ kv}$   
 $V_{arc} = 37 \text{ v}$        $V_- = -1.6 \text{ kv}$

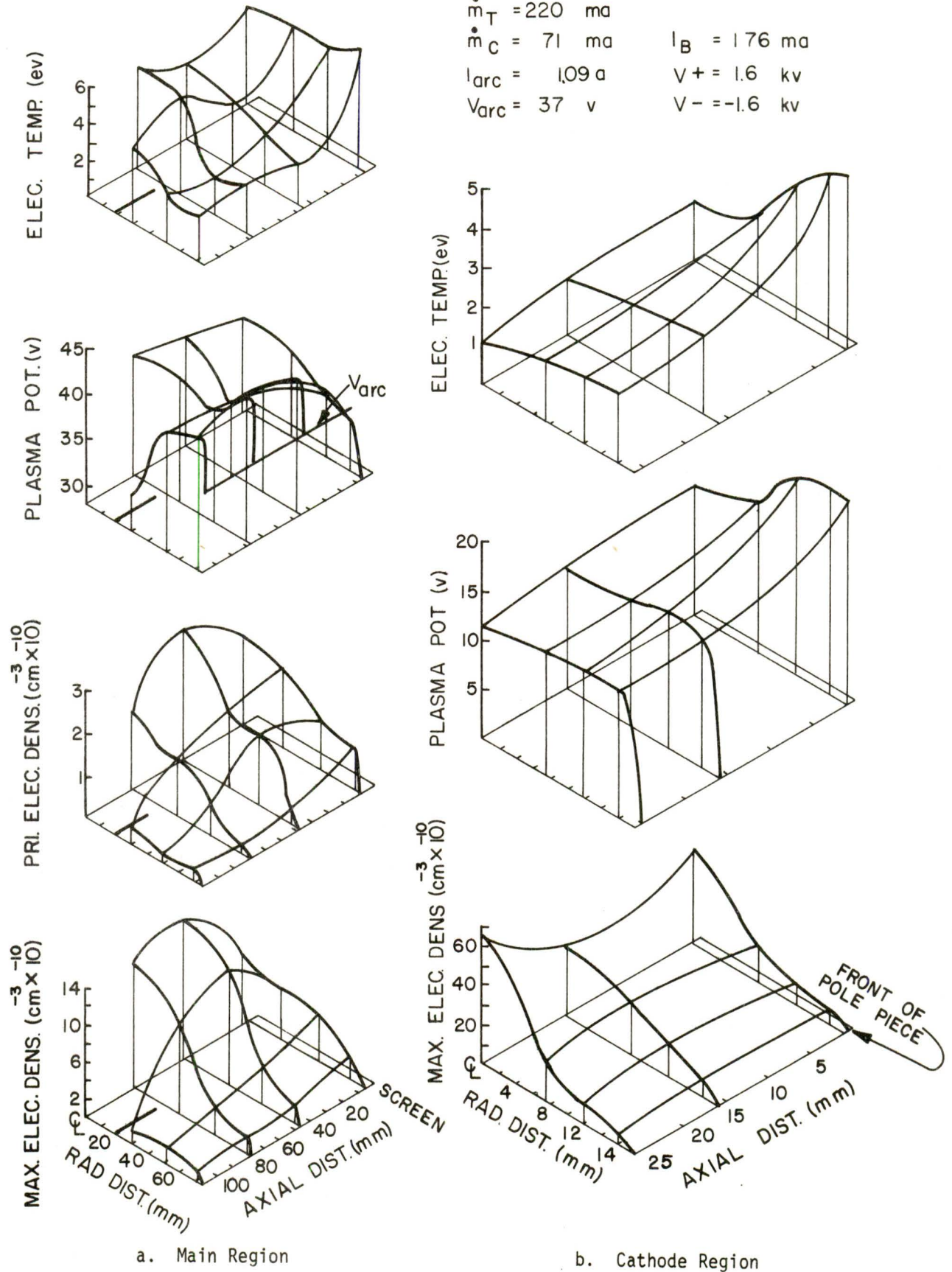
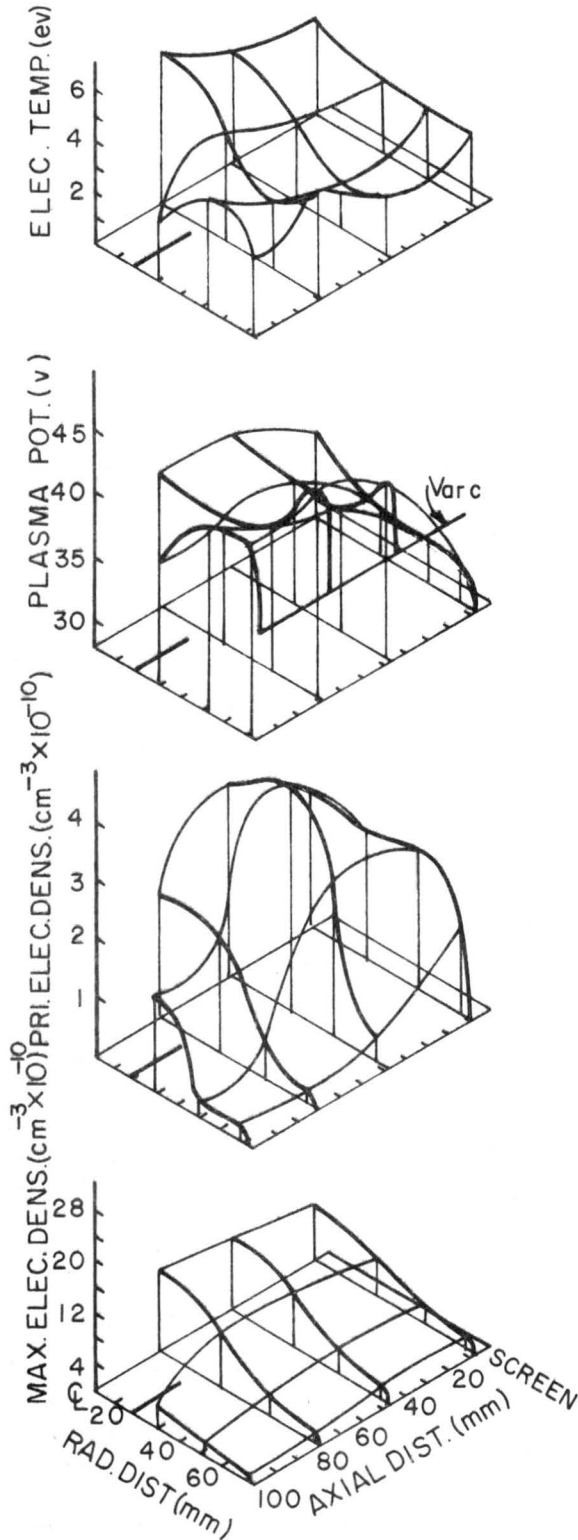
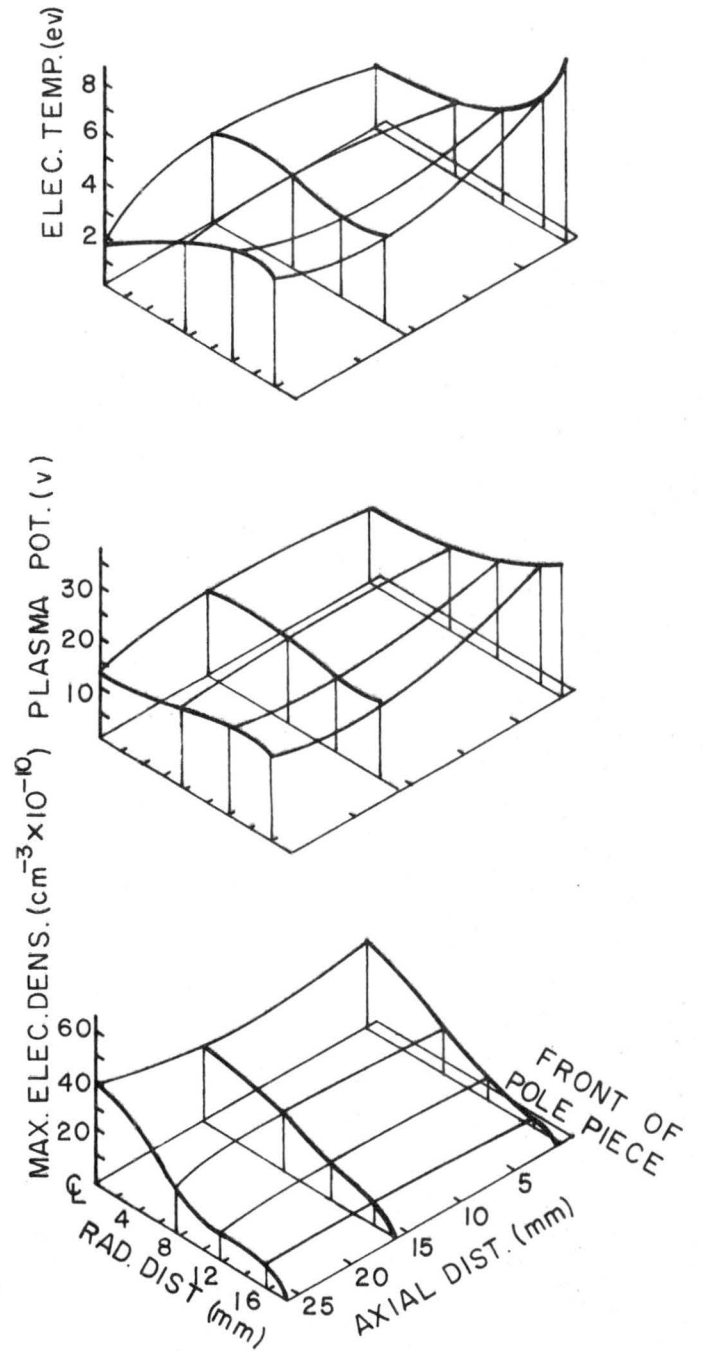


FIGURE 6.

$$\begin{aligned} \dot{m}_T &= 220 \text{ ma} & I_B &= 162 \text{ ma} \\ \dot{m}_C &= 110 \text{ ma} & V_+ &= 1.6 \text{ kv} \\ I_{arc} &= 1.22 \text{ a} & V_- &= -1.6 \text{ kv} \\ V_{arc} &= 37 \text{ v} \end{aligned}$$



a. Main Region

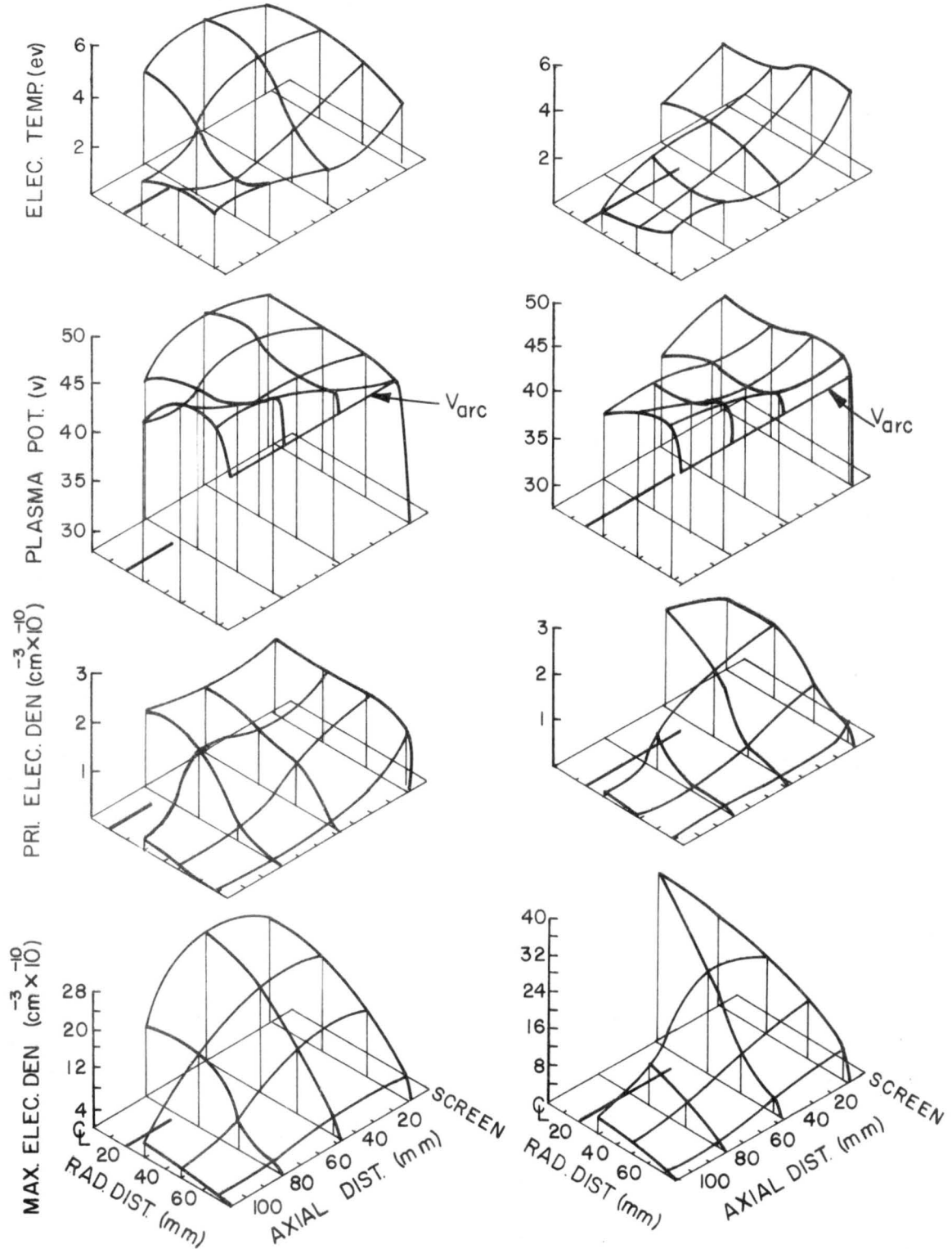


b. Cathode Region

FIGURE 7.

$\dot{m}_T = 440 \text{ ma}$   
 $\dot{m}_C = 112 \text{ ma}$      $I_B = 309 \text{ ma}$   
 $I_{arc} = 1.84 \text{ a}$      $V_+ = 1.6 \text{ kv}$   
 $V_{arc} = 43 \text{ v}$      $V_- = -1.6 \text{ kv}$

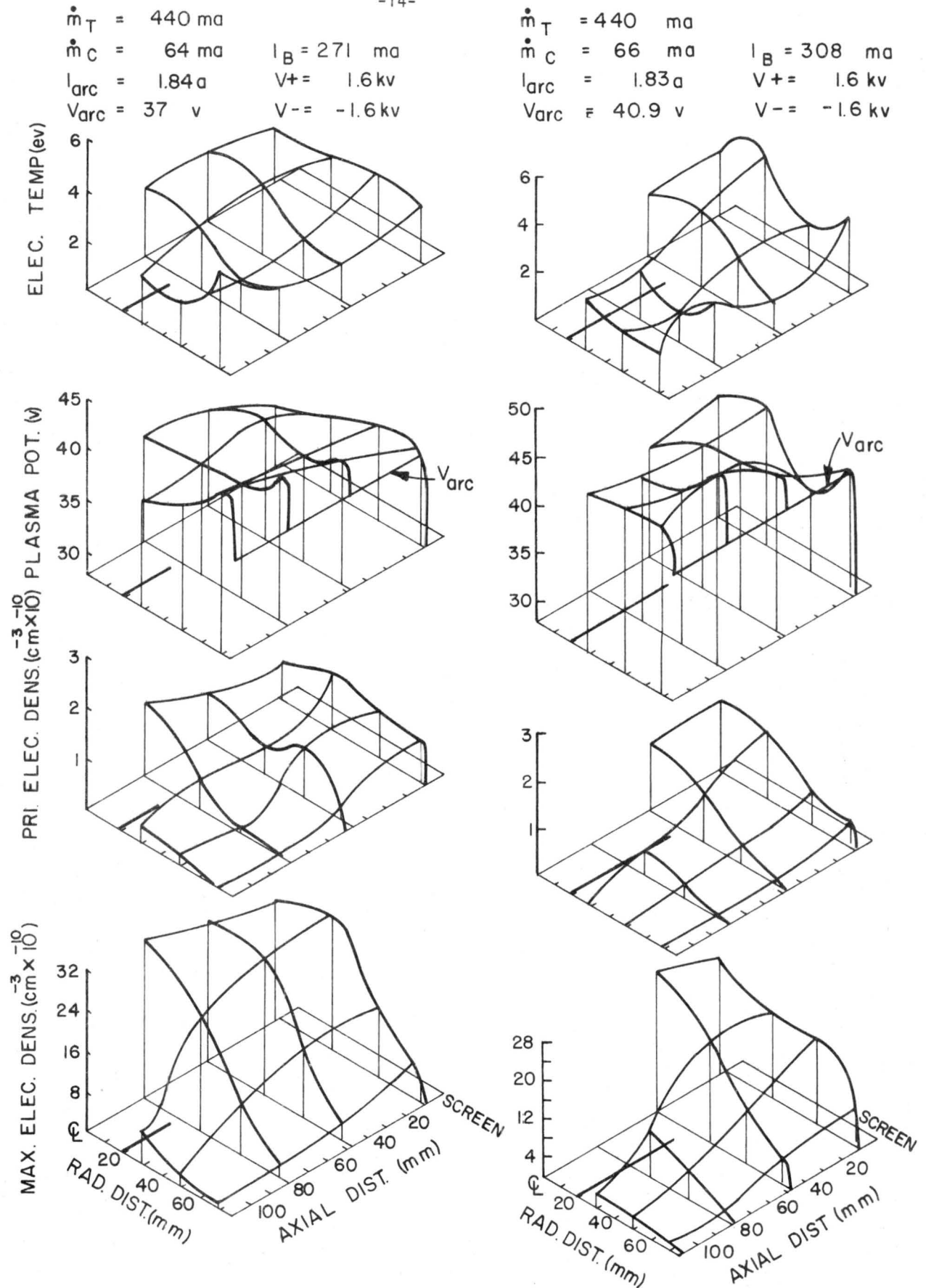
$\dot{m}_T = 440 \text{ ma}$   
 $\dot{m}_C = 114 \text{ ma}$      $I_B = 271 \text{ ma}$   
 $I_{arc} = 1.8 \text{ a}$      $V = 1.6 \text{ kv}$   
 $V_{arc} = 39.5 \text{ v}$      $V = -1.6 \text{ kv}$



a. Pole Piece Sleeve Flush

b. Pole Piece Sleeve Extended 3 cm

FIGURE 8.



a. Pole Piece Sleeve Flush

b. Pole Piece Sleeve Extended 3 cm

FIGURE 9.



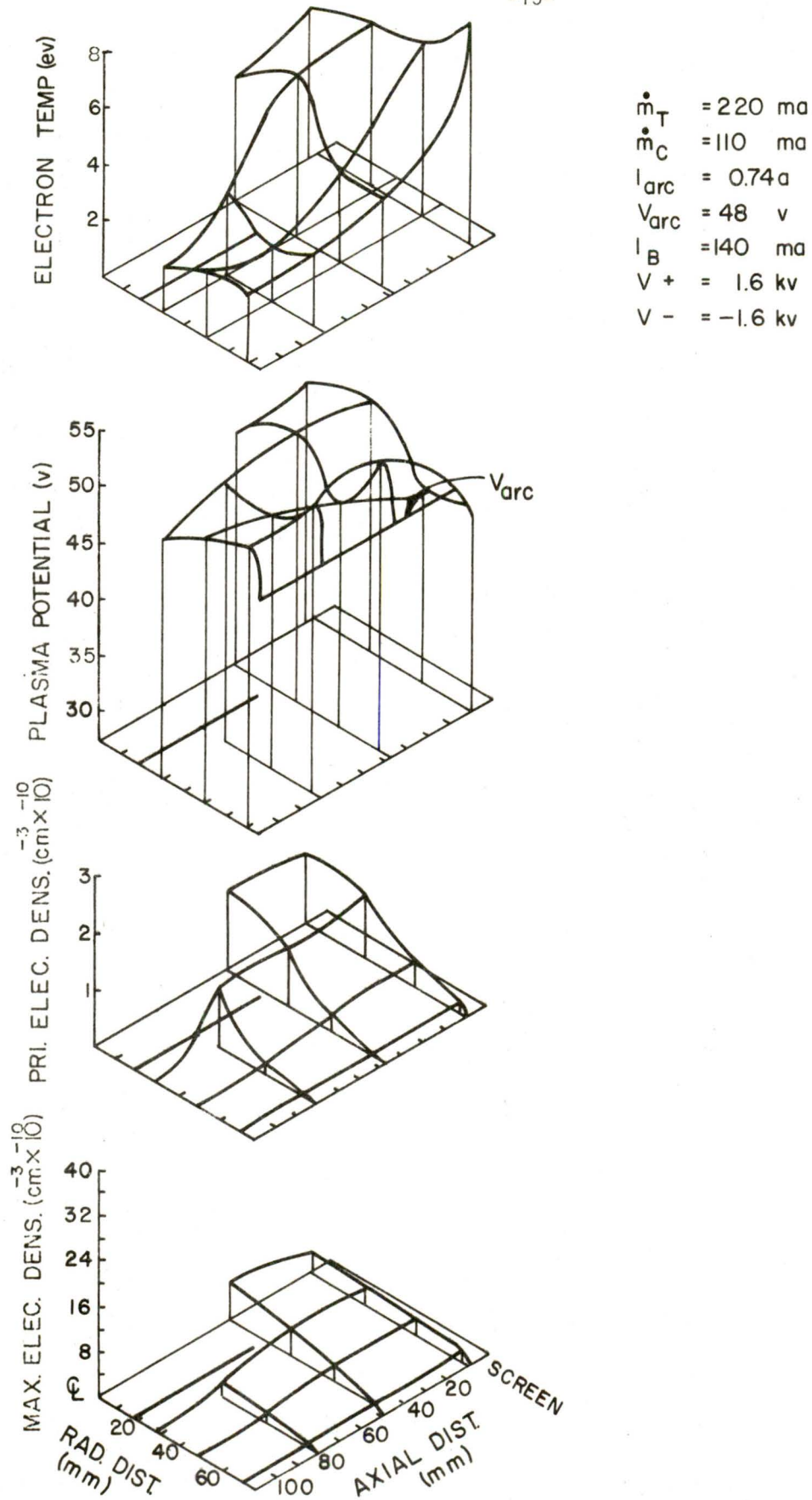
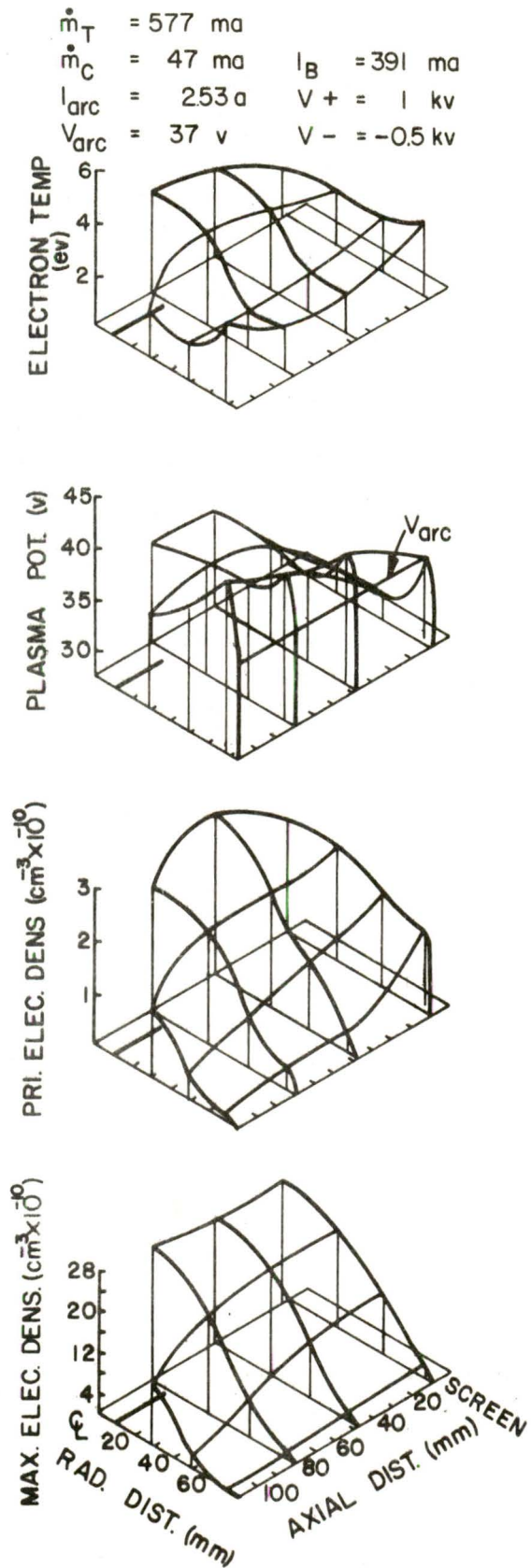
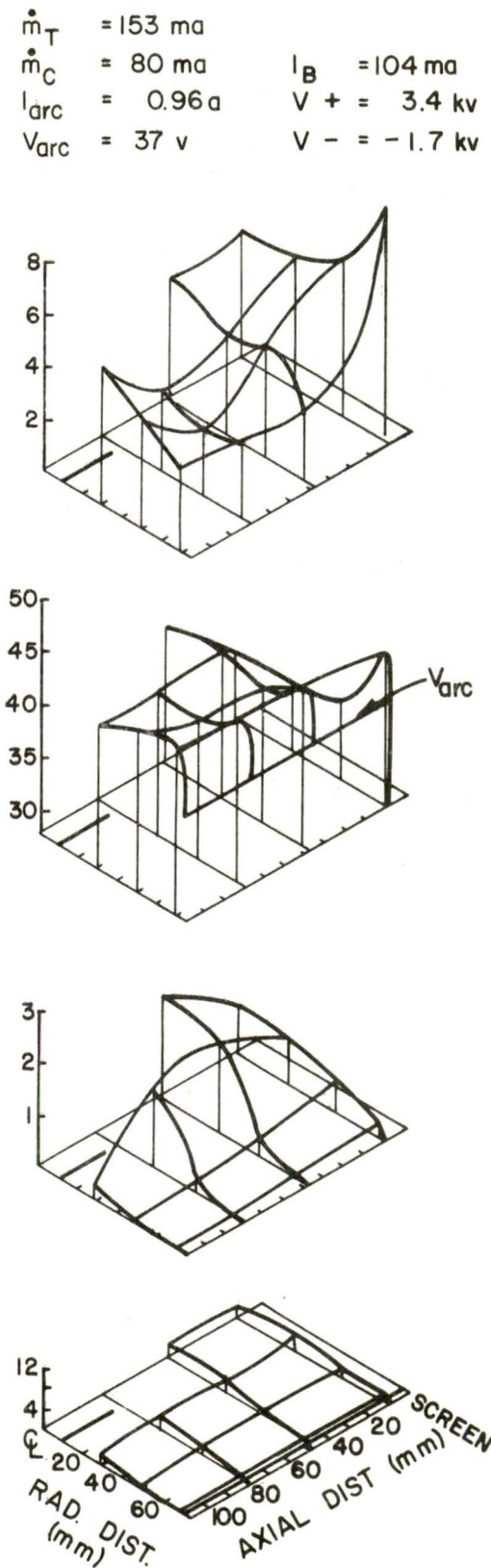


FIGURE 10. Pole Piece Sleeve Extended 3 cm



a. Dished Grid System  
High Flow Rate



b. Flat Grid System  
Low Flow Rate

FIGURE 11.



$\dot{m}_T = 688 \text{ ma}$   
 $\dot{m}_C = 10 \text{ ma}$       $I_B = 478 \text{ ma}$   
 $I_{arc} = 3.9 \text{ a}$       $V_+ = 1 \text{ kv}$   
 $V_{arc} = 33 \text{ v}$       $V_- = -0.5 \text{ kv}$

$\dot{m}_T = 686 \text{ ma}$   
 $\dot{m}_C = 51 \text{ ma}$       $I_B = 529 \text{ ma}$   
 $I_{arc} = 3.88 \text{ a}$       $V_+ = 1 \text{ kv}$   
 $V_{arc} = 34 \text{ v}$       $V_- = -0.5 \text{ kv}$

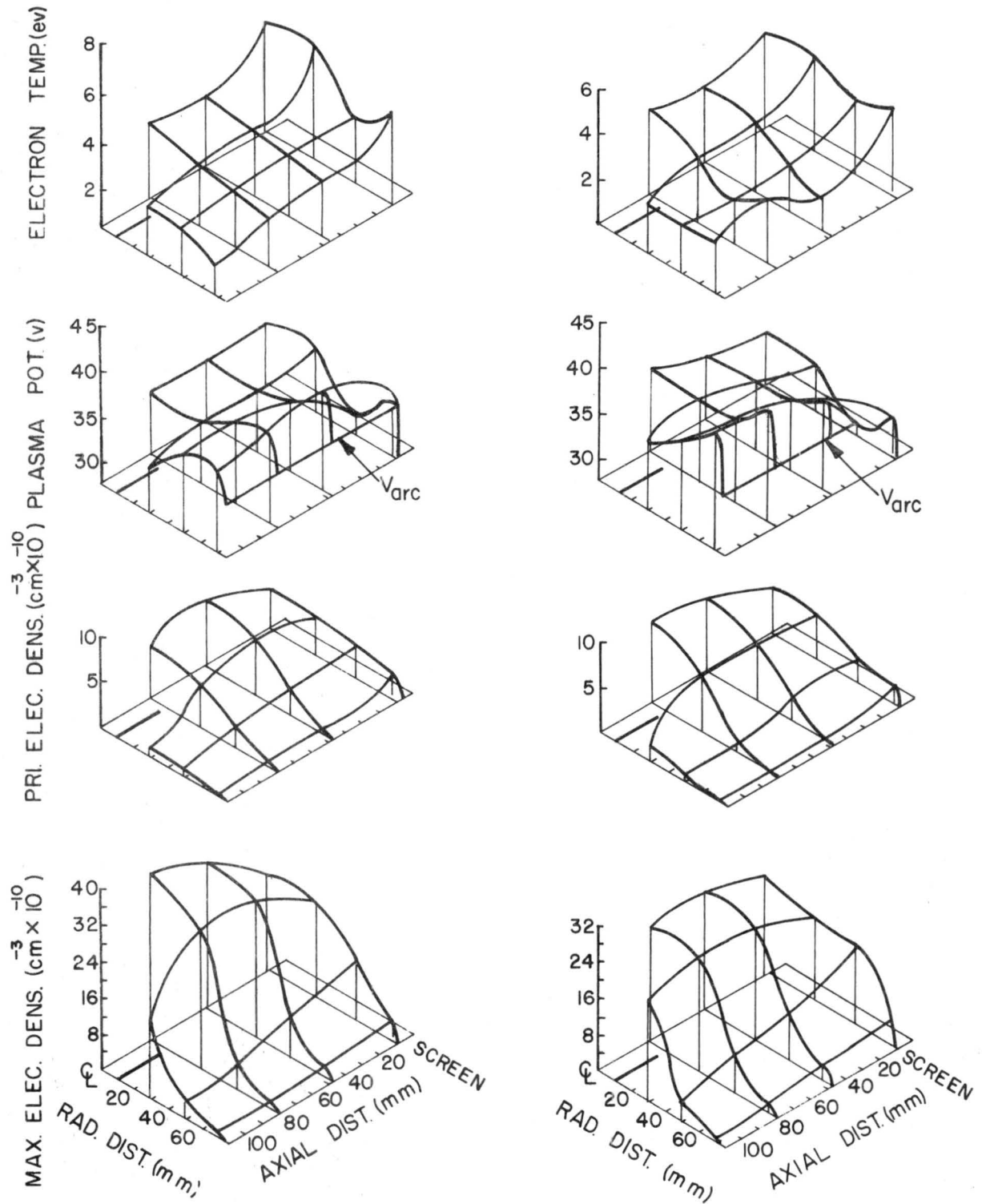


FIGURE 12. Dished Grid System - High Flow Cases

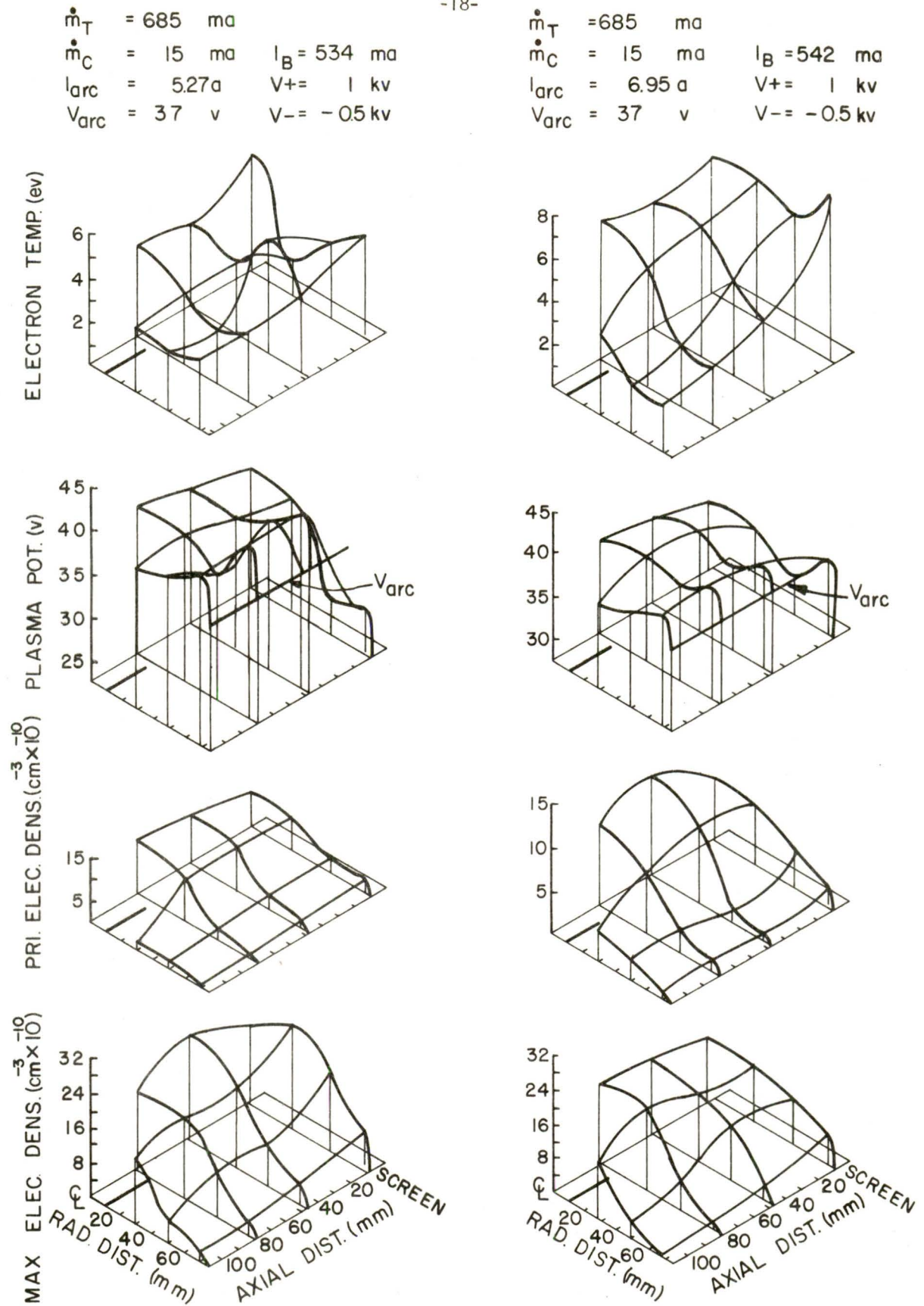


FIGURE 13. Dished Grid System - High Flow Cases

$\dot{m}_T = 131 \text{ ma}$   
 $\dot{m}_C = 75 \text{ ma}$       $I_B = 71 \text{ ma}$   
 $I_{arc} = 0.99 \text{ a}$       $V_+ = 1 \text{ kv}$   
 $V_{arc} = 37 \text{ v}$       $V_- = 0.5 \text{ kv}$

$\dot{m}_T = 220 \text{ ma}$   
 $\dot{m}_C = 75 \text{ ma}$       $I_B = 128 \text{ ma}$   
 $I_{arc} = 1.17 \text{ a}$       $V_+ = 1 \text{ kv}$   
 $V_{arc} = 37 \text{ v}$       $V_- = 0.5 \text{ kv}$

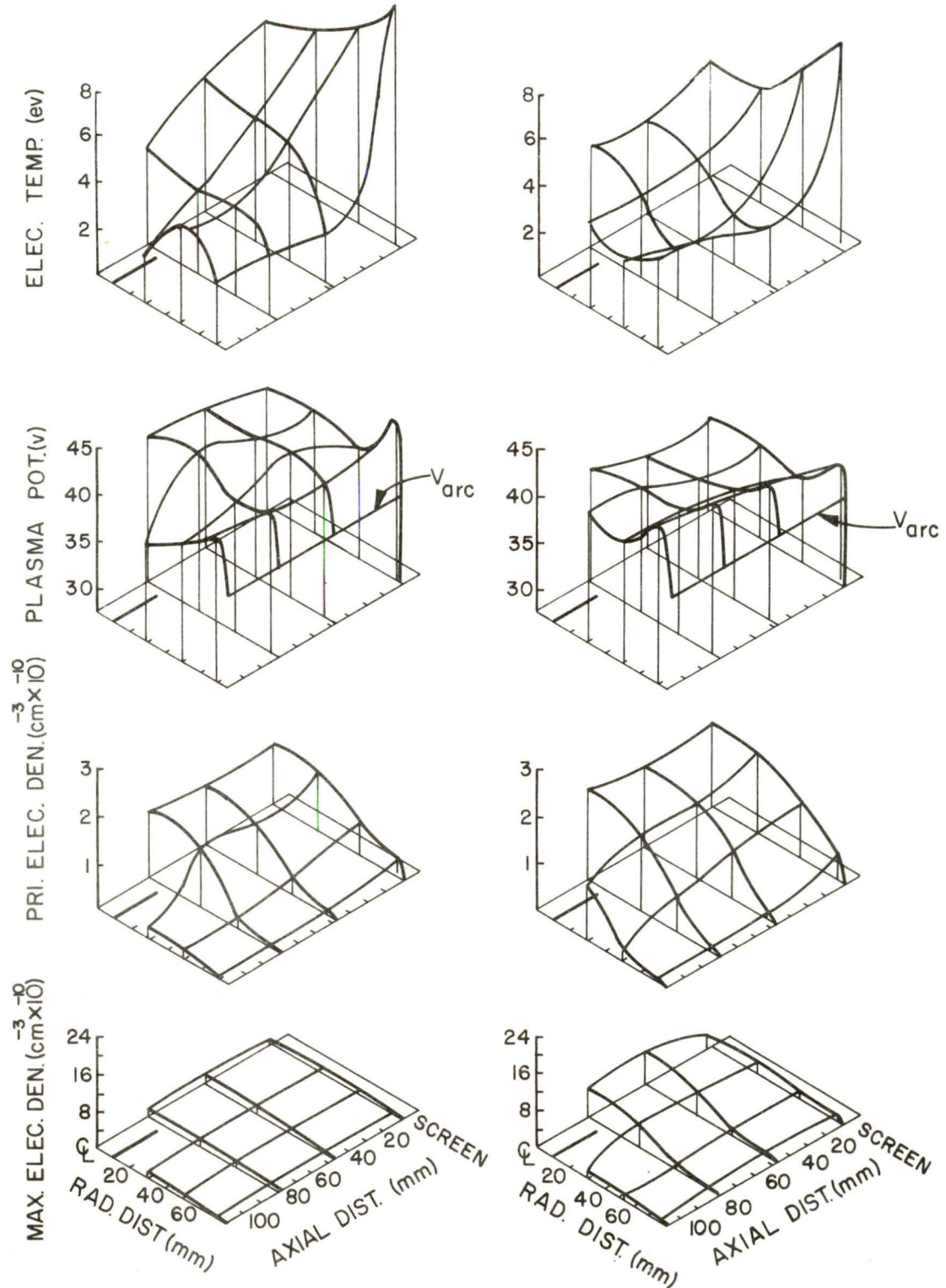


FIGURE 14. Dished Grid System - Low Flow Cases

REFERENCES

1. Wilbur, Paul J., "Experimental Investigation of a Throtttable 15 cm Hollow Cathode Ion Thruster," NASA CR-121038, December 1972.
2. Strickfaden, W. B. and K. L. Geiler, "Probe Measurements of the Discharge in an Operating Electron Bombardment Engine," AIAA Journal, Vol. 1, No. 8, pp. 1815-1822, August 1963.